In-flight absolute radiometric calibration of MODIS using the irradiance-based method

Wei Wei[1, 2*], Xin Li[1], Chun-yan Zhao[1], Gang-gang Qiu[1, 2], Xiao-bing Zheng[1]

[1]Key Laboratory of Optical Calibration and Characterization, Anhui Institute of Optics and Fine Mechanics, Chinese Academy of Sciences, Hefei 230031, China
[2]University of Science and Technology of China, Hefei 230026, China

ABSTRACT

In order to reduce the calibration uncertainty of the reflectance-based method brought by the assumption of the aerosol model, the irradiance-based method, known as improved reflectance-based method, was proposed. The irradiance-based method is described in this paper. The radiometric calibration field campaign was performed at Dunhuang test site on 27 August, 2014. A hyperspectral irradiance meter (HSIM) developed by Anhui Institute of Optics and Fine Mechanics (AIOFM) was used to measure the diffuse-to-global spectral irradiance ratio. The irradiance-based method and the reflectance-based method were performed to calibrate the first four bands of Moderate Resolution Imaging Spectroradiometer (MODIS). The results of two methods were compared with result of MODIS on-board calibrator. The comparison shows that the result of irradiance-based method has a good consistency with on-board calibration and reflectance-based method results. The difference of calibration coefficients between irradiance-based and on-board method was less than 1.4%. Due to the limitations of the irradiance-based method, a clear sky and stable atmospheric condition is required for the entire half of the calibration day to provide the data necessary for the extrapolation of diffuse-to-global ratio in viewing direction. A study on the effects of aerosol mode assumption on the final apparent reflectance was performed on both the irradiance-based method and the reflectance-based method by selecting different aerosol modes to predict the apparent reflectance. The results show that aerosol mode assumption has a great effect on the reflectance-based method, however slight effect on the irradiance-based method.

Keywords: radiometric calibration, irradiance-based method, diffuse-to-global ratio, MODIS

1. INTRODUCTION

With rapid development of quantitative remote sensing satellite technology and quantitative applications of remote sensing data, especially the use of quantitative multispectral remote sensing data acquired from various remote sensing satellites to monitor and predict the process of global climate change, the requirement to improve the accuracy of radiometric calibration of remote sensing sensor is increasingly urgent.[1] The radiometric calibration is the premise and basis of quantitative applications of remote sensing. Its aim is to stablish a relation between the output and the input of the remote sensing sensor. The accuracy of radiometric calibration directly affects the quality of quantitative remote sensing products.[2] Radiometric calibration method includes pre-launch calibration, on-orbit satellite calibration and in-flight vicarious calibration. Vicarious calibration is an effective method for the calibration of satellite sensor without on-board calibrator. In 1980s, Professor Slater proposed a method of using large-area uniform ground objects to achieve the in-flight vicarious absolute radiometric calibration of satellite sensor.[1] After the development of more than 30 years, test site vicarious calibration has become an operational method for a large number of remote sensing sensors' calibration. Test site vicarious calibration includes reflectance-based method, radiance-based method and irradiance-based method. The reflectance-based method uses the reflectance of ground target, spectral aerosol optical depth, meteorological parameters and the atmospheric radiative transfer model to calculate a radiance at the top of the atmosphere (TOA). The radiance is

* E-mail: wei1214@mail.ustc.edu.cn

Hyperspectral Remote Sensing Applications and Environmental Monitoring and Safety Testing Technology, edited by Wenqing Liu and Jinnian Wang, Proc. of SPIE Vol. 10156, 101561M · © 2016 SPIE · CCC code: 0277-786X/16/$18 · doi: 10.1117/12.2247217

compared to the digital number of the earth view data of the measured area to give a calibration coefficient.[3] For the radiance-based method, a well-calibrated radiometer is carried by an unmanned aerial vehicle flying over 3000 meters to measure the radiance of the ground target at the time of the satellite overpass with the same viewing geometry as the satellite sensor. The residual scattering and absorption between the radiometer and the satellite was removed from the measured radiance to calculate the TOA radiance. For the irradiance-based method, besides all of the measured data from the reflectance-based method, the diffuse-to-global ratio at the ground level is measured to compute the scattering. This additional measurement helps to reduce the calibration uncertainty contributed by the aerosol model assumption.[4]

The MODIS, currently operating on both the Terra and Aqua satellites, is one of the key instruments for NASA's Earth Observing System (EOS). It was designed and developed to obtain continuous global data for the researches of both short-term and long-term changes in the earth system. MODIS has its own excellent on-board calibration system, with a nice calibration accuracy of ±2% for the reflective solar bands (RSB) reflectance coefficients,[5] and it was often used as the reference sensor in the cross-calibration. This paper describes the method of irradiance-based method and the field campaign carried out in Dunhuang. Both irradiance-based and reflectance-based method were used to calibrate the first four bands of MODIS with the parameters measured at Dunhuang test site on August 27, 2014. The results of two method were compared with the MODIS on-board calibration coeffcients to validate the accuracy of the irradiance-based method.

2. IRRADIANCE-BASED METHOD

The radiance $L_\lambda(\theta_v, \theta_s, \varphi_v - \varphi_s)$ measured at the top of the atmosphere, at wavelength λ, can be expressed as an apparent reflectance:[6]

$$\rho_\lambda^*(\theta_v, \theta_s, \varphi_v - \varphi_s) = \frac{\pi L_\lambda(\theta_v,\theta_s,\varphi_v-\varphi_s)d^2}{E_{0\lambda}\mu_s}, \quad (1)$$

where $E_{0\lambda}$ is the exo-atmospheric solar spectral irradiance, θ_v, φ_v, θ_s and φ_s represents the observation and solar incidence and azimuth angles, d is the earth-sun distance in astronomical units, and $\mu_s = \cos\theta_s$. For a uniform lambertian ground surface of reflectance ρ, the apparent reflectance ρ^* can be described as:[6]

$$\rho^*(\theta_v, \theta_s, \varphi_v - \varphi_s) = T_g(\mu_v, \mu_s)[\rho_A(\theta_v, \theta_s, \varphi_v - \varphi_s) + \frac{\tau(\mu_s)\rho\tau(\mu_v)}{1-\rho s}], \quad (2)$$

where τ is the global atmospheric transmittance, ρ_A is the intrinsic reflectance of the atmosphere, s is the spherical albedo of the atmosphere and $T_g(\mu_v, \mu_s)$ is the gaseous transmission.The global transmittance can be described as:[6]

$$\tau(\mu_s) = e^{-\delta/\mu_s} + \frac{E_d^0}{\mu_s E_s}, \quad (3)$$

where E_d^0 is the downward irradiance at the ground level due only to scattering, δ is total atmospheric optical depth. Fig. 1 illustrates the composition of the irradiance at the ground level.[6]

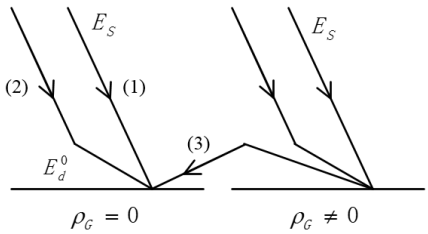

(1) Direct irradiance at ground level = $\mu_s E_s e^{-\delta/\mu_s}$ (2) Intrinsic atmospheric irradiance = E_d^0
(3) Coupled ground-atmosphere irradiance = $\mu_s E_s \frac{\tau(\mu_s)}{1-\rho s}$
Fig. 1. The composition of irradiance at the ground level[6]

As is shown in Fig. 1, the diffuse irradiance term $E_d(\mu_s)$ includes the intrinsic diffuse irradiance $E_d^0(\mu_s)$ and also the coupling term between the atmosphere and the ground for both the direct beam and the diffuse component for our measurement method. The diffuse irradiance can be expressed as:[6]

$$E_d(\mu_s) = \frac{E_d^0(\mu_s)+\mu_s E_s e^{-\delta/\mu_s}\rho s}{1-\rho s}, \tag{4}$$

and then we can get $\tau(\mu_v)$ as

$$\tau(\mu_s) = \frac{(1-\rho s)e^{-\delta/\mu_s}}{1-\alpha_s}. \tag{5}$$

According to the reciprocity principle, the transmittance in the view direction can be described as:[6]

$$\tau(\mu_v) = \frac{(1-\rho s)e^{-\delta/\mu_v}}{1-\alpha_v}, \tag{6}$$

where α_v is the ratio of diffuse-to-global irradiance measured in the viewing direction. And now we can rewrite the apparent reflectance as:[6]

$$\rho^*(\theta_v,\theta_s,\varphi_v-\varphi_s) = T_g(\mu_v,\mu_s)[\rho_A(\theta_v,\theta_s,\varphi_v-\varphi_s) + \frac{e^{-\delta/\mu_s}}{1-\alpha_s}\rho(1-\rho s)\frac{e^{-\delta/\mu_v}}{1-\alpha_v}]. \tag{7}$$

A radiative transfer code is needed to predict the apparent reflectance in the reflectance-based method using Equation 2. The aerosol optical depth derived from extinction measurements is a key input for the radiative transfer code. Several aerosol models with default aerosol refractive index and size distribution were presented to select to calculate the scattering phase function or matrix. The uncertainty of predicted apparent reflectance contributed by aerosol model selection is much more than the others. For the irradiance-based method, the apparent reflectance is computed using Equation 8. Only the values of ρ_A, s and $T_g(\mu_v,\mu_s)$ are computed using a radiative transfer code. It helps to reduce the uncertainty of apparent reflectance computation caused by the assumption of aerosol model.[6]

In order to perform the irradiance-based method calibration, target ground reflectance, aerosol optical depth, diffuse to global irradiance ratio and some meteorological parameters need to be measured at the time of satellite overpass. The flow chart of the irradiance-based method is shown in Fig. 2.

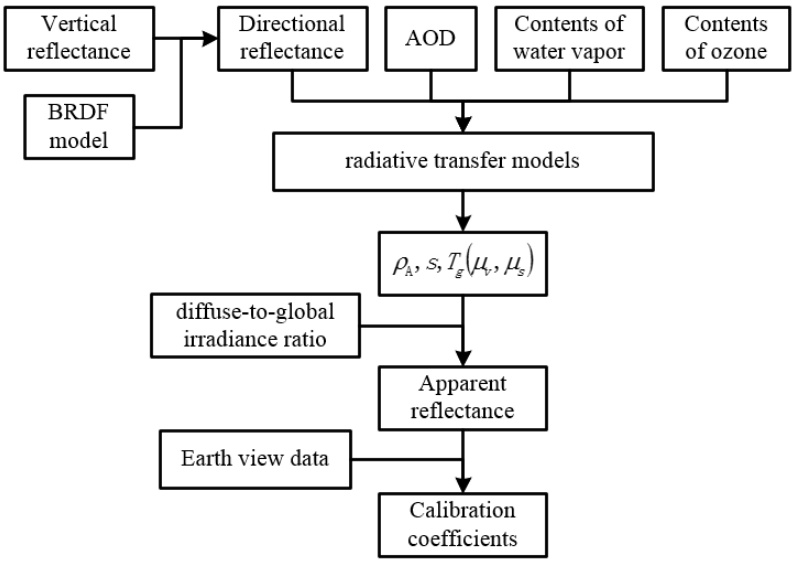

Fig. 2. Flow chart of irradiance-based calibration method

3. EXPERIMENT AND DATA PROCESS

3.1 Test site

Dunhuang test site is one of the Chinese Radiometric Calibration Sites (CRCS), located in the northwest of Dunhuang, Gansu province, China. It is an alluvial fan gobi of Danghe River, and covers an area of 25km × 25km. The surface of Dunhuang test site is relatively flat, composed by a variety of gravel, sand and a small amount of clay.[7] It has a nice spatial heterogeneity of less than 2% over its 10km × 10km central region.[8]

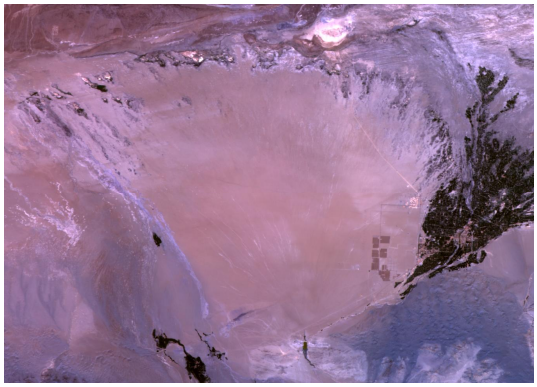

Fig. 3. Satellite image of Dunhuang test site

Fig.4. The surface of Dunhuang test site

3.2 Reflectance measurement

The 10km × 10km central region of Dunhuang test site was selected as the test area to obtain the ground reflectance. The geographic coordinates of the its northwest and southeast corner are (94.24°E, 40.20°N) and (94.40°E, 40.08°N). Totally 11 synchronous sample points were deployed in this region. An ASD FieldSpec3 spectral radiometer and a standard reference panel were used to measure the vertical reflectance at the time of satellite overpass. One time reference panel measurement, five times ground target measurement and one time reference panel measurement were performed in sequence at each sample point. The ASD and the reference panel have been calibrated in AIOFM before the field campaign.

Due to the non-Lambert characteristic of the surface, a Bidirectional Reflectance Distribution Function (BRDF) model AMBRALS supported by National Satellite Meteorology Center, China Meteorological Administration, was used to correct the reflectance in view direction. The AMBRALS model can be expressed as:[9]

$$\rho_{AMBRALS}(\theta_v, \theta_s, \varphi) = f_{iso} + f_{vol}k_{vol}(\theta_v, \theta_s, \varphi) + f_{geo}k_{geo}(\theta_v, \theta_s, \varphi) \ , \tag{8}$$

$$A(\theta_s) = \frac{\rho_{AMBRALS}(\theta_v, \theta_s, \varphi)}{\rho_{AMBRALS}(0, \theta_s, 0)} \ , \tag{9}$$

$$\rho_{direction}(\theta_v, \theta_s, \varphi) = A(\theta_s)\rho_{ASD}(0, \theta_s, 0) \ , \tag{10}$$

where, $\varphi = \varphi_v - \varphi_s$. $\rho_{AMBRALS}(\theta_v, \theta_s, \varphi)$ is the reflectance in the view direction calculated by the AMBRALS model when the sun is in the direction of (θ_s, φ_s). $k_{vol}(\theta_v, \theta_s, \varphi)$ and $k_{geo}(\theta_v, \theta_s, \varphi)$ are respectively the volume scattering kernel and geometrical optics scattering kernel only related to the viewing geometry. f_{iso}, f_{vol} and f_{geo} are the factors related to the kernels. $\rho_{AMBRALS}(0, \theta_s, 0)$ is the vertical reflectance calculated by the AMBRALS model. $\rho_{ASD}(0, \theta_s, 0)$ is the vertical reflectance measured by ASD. $\rho_{direction}(\theta_v, \theta_s, \varphi)$ is the ground reflectance in the view direction of (θ_v, φ_v) correected by the AMBRALS BRDF model.

The vertical reflectance measured by ASD and directional reflectance corrected by AMBRALS BRDF model of test area in August 27 are shown in Fig. 5. In order to obtain the MODIS band reflectance ρ_i, MODIS spectral response function $R(\lambda)$ is needed to have a convolution with the directional reflectance.

$$\rho_i = \frac{\int \rho_{direction}(\lambda) R(\lambda) d\lambda}{\int R(\lambda) d\lambda} \tag{11}$$

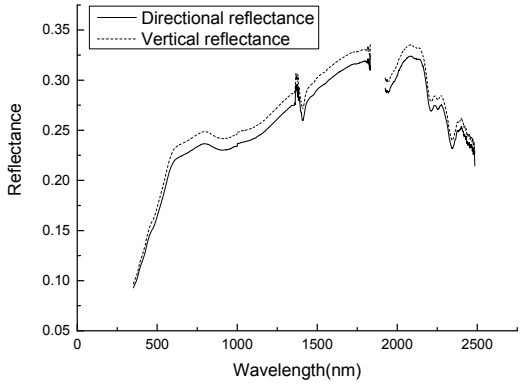

Fig. 5. Reflectance of test area on August 27
($\theta_s = 32.35,\ \varphi_s = 154.54,\ \theta_v = 17.28,\ \varphi_v = 281.43$)

3.3 Diffuse-to-global ratio measurement

Diffuse-to-global irradiance ratio is a key parameter of the irradiance-based method. It is used to characterize the atmospheric scattering. The HSIM was used to measure the diffuse-to-global ratio. The HSIM which is shown in Fig. 6 covers a wavelength range from 400nm to 2400nm. A black ball can automatically block the direct beam when measuring the diffuse irradiance. When the ball falls down, the global irradiance was measured. Then we can calculate the diffuse-to-global ratio. The ratio was measured every two minutes.

Fig. 6 Hyperspectral irradiance meter

MODIS spectral response function $R(\lambda)$ is used to have a convolution with the diffuse-to-global spectral ratio $\alpha(\lambda)$ to calculate the band diffuse-to-global ratio.

$$\alpha_i = \frac{\int \alpha(\lambda) R(\lambda) d\lambda}{\int R(\lambda) d\lambda} \tag{12}$$

The measured diffuse-to-global spectral ratio at the time of satellite overpass on August 27 is plotted in Fig. 7. From the reciprocity principle, we can obtain the upward global atmospheric transmittance using the measurements at the solar angle θ_s equal to the viewing angle. There are two limitations to this method. First, a clear sky and a stable atmosphere are needed between the time of overpass and the measurements. Second, for some high latitude places, it is necessary to

extrapolate to the actual view angle in certain cases as the range of solar zenith angle may never cover the view zenith angle. In this case, a knowledge of the relation of the diffuse-to-g1obal ratio versus the airmass can help us deduce the diffuse-to-global ratio in viewing direction.[6] The diffuse-to-global ratio has a linear relation with the airmass. The long time series diffuse-to-global ratios are needed to deduce the diffuse-to-global ratios in the viewing direction.

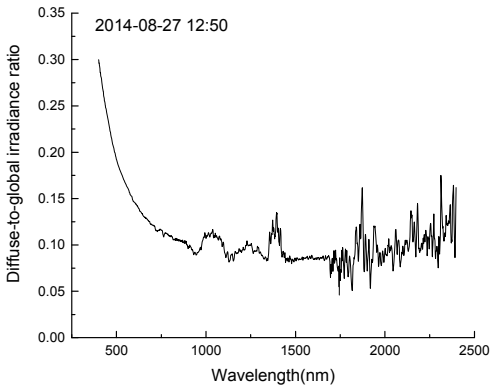

Fig. 7. Diffuse-to-global ratio at the time of satellite overpass

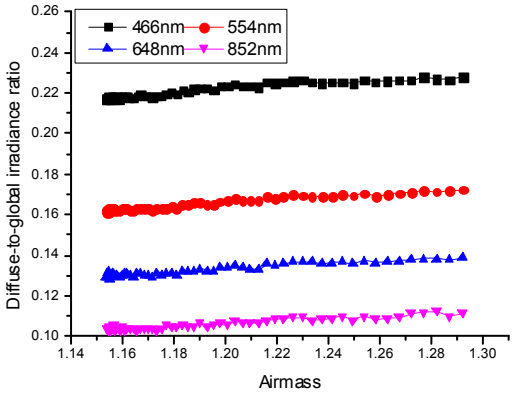

Fig. 8. Long time series diffuse-to-global ratios

3.4 Other parameters

The aerosol optical depth was measured by a sun photometer CE318. The water vapor concentration was calculated from radiosounding data. Ozone concentration was obtained from NASA's OMI product. The geometric condition and meteorological parameters needed for calibration are listed in Table 1.

Table 1. Geometric condition and meteorological parameters for calibration

Sensor	Overpass time (In UTC)	Solar zenith	Satellite zenith	H2O (g/cm2)	AOD (550nm)	O3 (DU)
Terra MODIS	2014-08-27 08:50	32.35	17.28	1.214	0.0974	285

4. RESULT AND ANALYSIS

The equivalent band reflectance, aerosol optical depth, total column water vapor, content of ozone, solar and viewing geometric condition were inputted into the atomspheric radiative transfer model, 6S, to calculate the atmospheric intrinsic reflectance ρ_A, spherical albedo s and the gaseous transmission $T_g(\mu_v, \mu_s)$. The desert model was selected to calculate these parameters. The assumption of the aerosol model only has affection on the atmospheric intrinsic reflectance and the spherical albedo. It helps to reduce the uncertainties in the scattering computations. Since all the parameters needed for the irradiance-based method were obtained, the apparent reflectance of MODIS band can be calculated using Equation (8). For the reflectance-based method, the apparent reflectance can be calculated directly using the atomspheric radiative transfer model. For the MODIS RSB, since the offset of MODIS first seven bands were 0, a simple linear algorithm is used as:[5]

$$\rho_i^* \cdot \mu_s / d^2 = A_i \cdot DN_i, \tag{13}$$

where ρ_i^* is the equivalent band apparent reflectance, DN_i is the sensor's earth view digtal number, and A_i is the reflectance calibration coefficient. Both the irradiance-based method and reflectance-based method are used to calculate the calibration coefficient. The results of two methods are listed in Table 2.

Table 2. Results of calibration

Band	1	2	3	4
A_i from irradiance-based method/$\times 10^{-5}$	5.514	3.310	5.636	4.480
A_i from reflectance-based method/$\times 10^{-5}$	5.484	3.249	5.455	4.404
A_i from on-board method/$\times 10^{-5}$	5.576	3.354	5.576	4.459
Error between irradiance-based and reflectance-based method (%)	0.544	1.843	3.211	1.696
Error between irradiance-based method and on-board method (%)	-1.114	-1.313	1.079	0.458
Error between reflectance-based method and on-board method (%)	-1.651	-3.144	-2.172	-1.238

As is shown in Table 2, the calibration coefficients of irradiance-based method and reflectance-based method were in good agreement with an error less than 3.3%, and both the two method coefficients were in good agreement with the on-board coefficients. The error between reflectance-based and on-board method was less than 3.2%, and the error between irradiance-based and on-board method was less than 1.4% which confirmed the validity and the accuracy of the irradiance-based method.

A study on the effects of aerosol mode assumption on the final apparent reflectance was performed on both the irradiance-based method and the reflectance-based method by selecting different aerosol modes to predict the apparent reflectance.[10] Continental model, desert model, urban model and Maritime model were used to estimate the apparent reflectance based on the measurement data at Dunhuang test site on August 27, 2014. We compared the apparent reflectance computed by irradiance-based and reflectance-based method using the four aerosol models. The result was illustrated in Fig. 9.

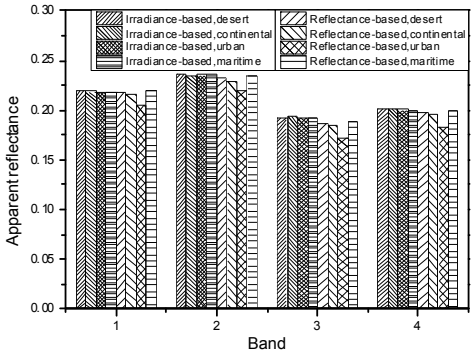

Fig. 9. Comparison of apparent reflectance between irradiance-based and reflectance-based method from four aerosol model

As is shown in Fig. 9, aerosol mode assumption has a great effect on the reflectance-based method, however slight effect on the irradiance-based method. The apparent reflectance of reflectance-based method using urban model is smaller than the others obviously. The difference of the apparent reflectance computed by irradiance-based method for four aerosol models varied from 0.02% to 0.95%. However for reflectance-based method, the difference of the apparent reflectance varied from 0.59% to 8.38%. It confirmed that irradiance-based method can reduce the uncertainty of calibration brought by aerosol model assumption.

5. CONCLUSION

A field campaign was carried out in Dunhuang test site. Both irradiance-based method and reflectance-based method were used to calibrate the Terra MODIS. The results of two method are in good consistency. And both results are in good agreement with the on-board calibration result. The difference of calibration coefficients between irradiance-based and

on-board method was less than 1.4% in the first four bands. It proved that the irradiance-based method can be used for the operational application of in-flight calibration.

The diffuse-to-global spectral ratio used for atmospheric transmittance computation was measured by the HSIM. Compared to the priviously measurement with radiometer and referance panel, it improved the accuracy of this measurement. An accurate measurement of diffuse-to-global ratio is a key factor to ensure accuracy of the absolute radiometric calibration. For the irradiance-based method, only ρ_A and s are affected by the assumption of aerosol model. It helps to reduce the calibration uncertainty caused by the assumption of aerosol model. Since there are some limitations in the irradiance-based method, a clear sky and stable atmospheric condition is required for half of the calibration day to provide the data necessary for the extrapolation of diffuse-to-global ratio in viewing direction. A study on the effects of aerosol mode assumption on the final apparent reflectance was performed on both the irradiance-based method and the reflectance-based method by selecting different aerosol modes to predict the apparent reflectance. The results show that aerosol mode assumption has a great effect on the reflectance-based method, however slight effect on the irradiance-based method.

ACKNOWLEDGEMENT

The authors would like to thank National Satellite Meteorology Center, China Meteorological Administration for providing observation data. This article was supported by the National Natural Science Foundation of China (No. : 41271373).

REFERENCES

[1] Qiu K. M., "The construction, scientific and technology production and its application foreground of China radiometric calibration site for remote sensing satellite," [The scientific and technology production papers florilegium of China Radiometric Calibration Sites for Remote Sensing Satellite], Ocean Press, Beijing, 2-10 (2001).
[2] Gong H., Tian G. L., Yu T., Zhang Y. X., Gu X. F. and Gao H. L., "Irradiance-based calibration and validation of MODIS visible and near-infrared channels," Journal of Remote Sensing, 14(2), 207-218 (2010).
[3] Slater P. N., Biggar S. F., Holm R. G., Jackson R. D., Mao Y., Moran M. S., Palmer J. M. and Yuan B., "Reflectance- and radiance-based methods for the cross absolute calibration of multispectral sensors," Remote Sensing of Environment, 22(1), 11-37 (1987).
[4] Biggar S. F., Dinguirard M. C., Gellman D. I., Henry P., Jackson R. D., Moran M. S. and Slater P. N., "Radiometric calibration of SPOT 2 HRV - A comparison of three methods," Proc. SPIE 1493, 155-162 (1991).
[5] Xiong X. X., Barnes W., "An overview of MODIS radiometric calibration and characterization," Advance in Atmospheric Sciences, 23(1), 69-79 (2006).
[6] Biggar S. F., "In-flight methods for satellite sensor absolute radiometric calibration," Dissertation of Ph.D., Tucson: University of Arizona (1990).
[7] He J. T., Lu Y. H., "The measurement and evaluation of bidirectional reflectance characteristics of Dunhuang Radiative Calibration site," Journal of Remote Sensing, 1(4), 246-251 (1997).
[8] Li Y., Rong Z. G., Zhang L. J. Sun L. and Xu N., "The comparison of BRDF model and validation of MCD43 products by the 2013 Dunhuang Gobi experiments," Proc. SPIE 9264, 926415-1 (2014).
[9] Li Y., Rong Z. G., Zheng Z. J., Liu J. J. Zhang L. J., Zhang L. Y., Hu X. Q., Zhang Y. and Sun L., "Post launch site calibration of visible and near-infrared channels of FY-3A visible and infrared radiometers," Optics and Precision Engineering, 17(12), 2966-2974 (2009).
[10] Hu X. Q., Zhang Y. X. and Qiu K. M., "In-flight Radiometric Calibration for VIR Channels of FY-1C Satellite Sensor by Using Irradiance-based Method," Journal of Remote Sensing, 7(6), 458-464 (2003).